INTERNATIONAL JOURNAL OF PRECISION ENGINEERING AND MANUFACTURING Vol. 16, No. 6, pp. 1171-1177 JUNE 2015 / 1171
DOI: 10.1007/s12541-015-0151-9 ISSN 2234-7593 (Print) / ISSN 2005-4602 (Online)

In Vivo Evaluation of the Subject-Specific Finite Element Model for Knee Joint Cartilage Contact Area

Kyoung-Tak Kang[1,*], Sung-Hwan Kim[2,*], Juhyun Son[1], Young Han Lee[3], and Heoung-Jae Chun[1,#]

1 Department of Mechanical Engineering, Yonsei University, 50 Yonsei-ro, Seodaemun-gu, Seoul, 120-749, South Korea
2 Department of Orthopedic Surgery, Arthroscopy and Joint Research Institute, Yonsei University College of Medicine, 50-1 Yonsei-ro, Seodaemun-gu, Seoul, 120-752, South Korea
3 Department of Radiology, Research Institute of Radiological Science, Medical Convergence Research Institute, and Severance Biomedical Science Institute, Yonsei University College of Medicine, 50-1 Yonsei-ro, Seodaemun-gu, Seoul, 120-752, South Korea
Corresponding Author / E-mail: hjchun@yonsei.ac.kr, TEL: +82-2-2123-4827, FAX: +82-2-362-2736
*Kyoung-Tak Kang and Sung-Hwan Kim contributed equally to this work

KEYWORDS: Finite element analysis, In vivo validation, Subject-specific knee model, Weight-bearing MRI

In this paper, we present a new validation method for subject-specific finite element (FE) modeling of the knee joint based on in vivo computed tomography (CT) and magnetic resonance imaging (MRI) data. Previously, several FE models have been developed for estimating the mechanical response of joint structures, where direct or indirect in vivo measurement is difficult or impossible. More recently, studies using MRI have provided clear visualization of the motion and deformation of the articular cartilage within the tibiofemoral (TF) joint space. Two methods have been introduced to validate in vivo subject-specific models: alignment of supine MRI with X-ray images and weight-bearing MRI. The size of the contact area between the femur and tibia was determined by computing the area of femoral cartilage that intersected the tibial cartilage. The result showed good agreement between non-weight bearing image aligned with X-ray and weight-bearing MRI images. This study may help to better define the relative importance of modeling validations for the development of subject-specific models.

Manuscript received: January 5, 2015 / Revised: March 12, 2015 / Accepted: March 12, 2015

1. Introduction

Contact pressure increases or alterations in knee joint structure and contact area are critical causes of knee pain and osteoarthritis.[1] Proper understanding and evaluation of knee joint biomechanics are therefore essential to improve the prevention and treatment of related disorders and injuries. Although this is an active area of research, the exact mechanical behavior of the knee joint and the causes of knee joint injury have not been completely elucidated. This is partially due to the inherent limitations of experimental studies such as high cost, difficulties associated with obtaining accurate measures of strain and stress, and challenges associated with the reproduction of certain natural, pathological or degenerative situations. Finite element (FE) models have been shown to provide insight into the mechanical properties of biological tissues and the performance of living organs, reducing both cost and time. Appropriately developed FE models are powerful tools to predict the effects of different parameters involved in knee pain and joint degradation and to provide information otherwise difficult to obtain from experiments. Magnetic resonance imaging (MRI) is considered to be an increasingly important tool for *in vivo* studies of musculoskeletal biomechanics. It can non-invasively obtain accurate geometric and anatomical information for both normal and injured joints. This information can be coupled with other analysis and modeling tools such as gait analysis and FE modeling to test hypotheses regarding joint function and the effects of injuries.[2] Recent advances in the field of medical imaging and its reconstruction have increased the potential to incorporate accurate tissue morphology and boundary conditions into *in vivo* subject-specific models.[3] Previous *in vivo* knee joint FE models have not sufficiently considering the functional joint kinematics involved in the joint-loading process.[4] Most of these studies have been validated or verified with published cadaveric testing references followed by *in vivo* FE modeling.[5-8] Furthermore, a method of subject-specific modeling has been introduced using MRI data from cadavers, validated using subject-specific cadaver testing.[9] Validation or verification is a crucial step before interpreting model predictions or using the model for clinical applications.[10,11] Beillas et al. used X-ray imaging that required surgical implantation of radio-opaque markers into the bone.[12,13] Yao et al. utilized a loading device to exert a force on the knee as it was undergoing MRI in a supine position.[14] Carey et al. have developed a technique to validate

the FE model in vivo using dynamic stereo-radiography data.[15] However, it requires a dual-fluoroscopy apparatus or weight-bearing MRI. The present FE study is cost effective and efficient and allows us to resolve problems as they develop, which is not generally the case in experimental studies.

Here, we presented a complete 3D subject-specific FE model of the healthy human knee joint including all relevant ligaments, menisci and articular cartilages. We developed a new subject-specific FE model for *in vivo* validation, which is more economic and user-friendly than conventional models. First, 3D weight-bearing images were developed by combining 2D X-ray and supine MRI images. The intersection area between tibiofemoral (TF) articular cartilages was considered to be the contact area. Second, weight-bearing MRI of the TF knee was examined. Finally, the subject-specific FE model developed from non-weight bearing MRI images was used to validate the two techniques mentioned above.

Fig. 1 Axial loading experiment apparatus mounted on the magnetic resonance imaging table

2. Materials and Methods

2.1 Magnetic resonance imaging-based axial loading experiment

After authorization from the hospital's institutional review board, subject-specific data was used to develop the FE model and *in vivo* validation method. One healthy male subject without a history of knee injury or patellar subluxation participated in this study (34 years, 178 cm, 75 kg). The subject was positioned supine with his right knee at full extension in an axial loading device (Fig. 1). Images were acquired using a 3.0 Tesla MRI scanner (Achieva 3.0T; Philips Healthcare, Netherlands) and a custom designed knee joint cadio coil. The axial-loaded supine MRI technique was first described by Willen et al.[16] The technique is based on the use of an MRI-compatible positioning device that compresses the knee joint axially between the shoulder and foot while the subject is in a supine position. The non-magnetic device consists of a harness and a foot-operated compression device connected by side straps (DynaWell Int., AB, Billdal, Sweden). An MRI-compatible device for loading the spine (DynaWell) was modified to allow resistive quadriceps force at preset knee flexion angles (Fig. 1). The side straps could be tightened to provide axial load on the knee joint, with the subject in the supine position with extended hips and knees. The axial load was regulated by tightening or loosening adjustment knobs on the foot-compression device. The harness was constructed to ensure that pressure was evenly distributed across the lower parts of the shoulders. The DynaWell device was used in combination with conventional closed configuration magnets, and the device was designed for imaging of the knee joint under axial loading (Fig. 1). The subject was instructed to push his feet against the footplates to generate an equivalent ground reaction force.[17] MRI scans were obtained at 0.4 mm slice thickness in the sagittal plane. High resolution setting were used for the spectral presaturation inversion recovery (SPIR) sequence (TE: 25.0 ms, TR: 3,590.8 ms, acquisition-matrix: 512×512 pixels, NEX: 2.0, field-of view: 140×140 mm).

2.2 Finite element analysis

A 3D FE model of a healthy lower extremity was developed from computed tomography (CT) images obtained with a light-speed volume

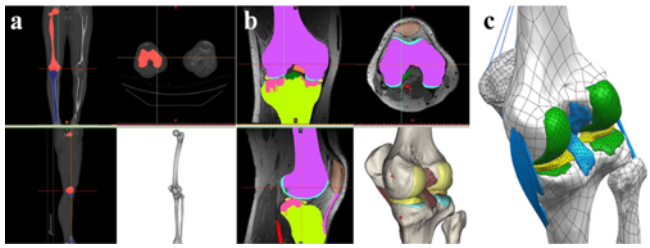

Fig. 2 Methodology for the 3D modeling of the intact knee: (a) 3D bone reconstruction; (b) 3D soft tissue and ligament reconstruction; (c) 3D model modification

CT scanner (VCT; GE Medical Systems, Milwaukee, WI, USA). CT scanning was performed with 0.1 mm slices from the same supine MRI subject. Digital CT data was imported into Mimics software (version 14.1; Materialise, Leuven, Belgium), which was used to generate the 3D geometrical surfaces of the femur, tibia, fibula, and patella at full extension (Fig. 2). The models of the medial and lateral menisci, femoral cartilage, and eight major ligaments were developed manually in 3D reconstruction models based on MRI (Fig. 2).

The MRI data was used to reconstruct the femur with a distal thickness of 10.2 cm and the tibia with a proximal thickness of 7 cm. To match the positional coordinates of each model, the central point of the diaphysis of the femur, the midpoint of the trans-epicondylar axis, and the intercondylar notch were defined as anatomical reference points in the reconstructed CT and MRI models. The process of combining the reconstructed CT and MRI models with the positional alignment for each model was achieved with Rapidform commercial software (version 2006; 3D Systems Korea, Inc., Seoul, South Korea). The initial graphics exchange specification (IGES) files exported from Mimics were entered into Unigraphics NX (version 7.0; Siemens PLM Software, Torrance, CA, USA) to form solid models for each femur, tibia, fibula, patella and soft tissue segment (Fig. 2). The solid model was then imported into Hypermesh (version 8.0; Altair Engineering, Inc., Troy, MI, USA) to generate an FE mesh that was then analyzed with ABAQUS software (version 6.11; Simulia, Providence, RI, USA).

This model assumed that the bones were rigid structures because

bone is stiffer than relevant soft tissues; this assumption had minimal influence in the study results.[18] Therefore, each bony structure (femur, tibia, fibula, and patella) was represented as a primary node located at its center of rotation at full extension. FE models of the soft tissue included the articular, menisci, cartilage, and all eight major ligaments. The articular cartilages were defined as isotropic, linear elastic materials with a Young's modulus of 15 MPa and a Poisson's ratio of 0.47, simulating the time-independent and simple compressive load applied to the knee joint.[19] The menisci were modeled as transversely isotropic, linearly elastic, homogeneous material with a Young's modulus of 120 MPa in the circumferential direction and 20 MPa in the axial and radial directions. Poisson's ratio was 0.2 in both the circumferential and radial directions and 0.3 in the axial direction.[20-22] To simulate meniscal attachments, each meniscal horn was fixed to bone using linear spring elements (element type = SPRINGA) with a total stiffness of 2,000 N/mm at each horn.[23, 24] The interfaces between the cartilage and bones were modeled as fully bonded. Contact was modeled between the femoral cartilage and the meniscus, the meniscus and the tibial cartilage, and the femoral and tibial cartilage for both the medial and lateral sides, resulting in six contact pairs. We considered a full large-strain formulation, while the contact conditions in the model were general and included finite sliding. A kinematic constraint on contact overclosure was approximated so that the nodes on the slave surface did not penetrate into the master surface. The model was completed using the linear penalty method, which provided the value of contact stress at each surface node. The coefficient of surface friction was 0.02, which is in the normal range of friction of human articular joints.[25] Eight of the primary non-weight-bearing soft tissue structures crossing the TF joint were included: the anterior and posterior cruciate ligaments, medial and lateral ligaments, popliteal fibular ligament (PFL), oblique popliteal ligament (OPL), and medial and lateral posterior capsules, as shown in Fig. 2(b). Attachment sites for the cruciate and collateral ligaments were determined from the interface between the extracted 3D ligament contours and bony surfaces, while placement of the PFL and OPL were determined from literature descriptions.[26,27] The eight major ligament models were defined as hyperelastic rubber-like materials that perform nonlinear stress-strain relations.[28,29] A hyperelastic model is generally used in engineering to represent large, incompressible deformation. The model is characterized by a strain energy potential function represented by equations.[29] The polynomial form of the strain energy potential equation was chosen from the ABAQUS material library. Biological soft tissues are exposed to a distribution of *in vivo* residual stresses as a consequence of continuous growth, remodeling, damage, and viscoelastic strains. The initial ligament strain model was developed on the basis of the results of a previous study.[18]

Mesh convergence tests were performed to complete the simulation. Convergence was reached if the relative change between two adjacent meshes was less than 5%. Average element sizes were 0.8 mm for cartilage and menisci.

2.3 3D reconstruction reproducibility analyses

To evaluate inter-observer reproducibility, two trained observers segmented the MRI images of knee joint and developed cartilage and menisci models. The first observer (K.-T. Kang) had previous experience segmenting the articular cartilage for about 150 sets of knee MRI images, and the second observer was an orthopedic surgeon (S.-H. Kim) who had previously segmented 30 sets of knee MRI images. Average thicknesses were calculated for the same supine and weight-bearing regions for all of the cartilage and menisci models developed. The two observers were trained in the rule-based protocol including prior instruction of common rules between observers in 3D reconstruction and performed the same segmentation and reconstruction processes on the MRI images.[30] The average thicknesses from the same supine and weight-bearing regions were compared. Coefficient of variation (CV, %) was calculated for the 30 regions of cartilage and five regions of menisci. For comparison with other studies, the CV of the total cartilage and menisci volume was also calculated.

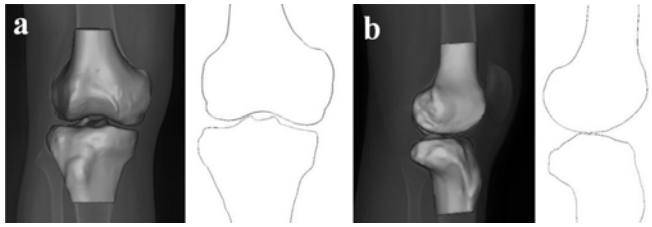

Fig. 3 Alignment of X-ray and supine MRI data using an iterative closet point algorithm

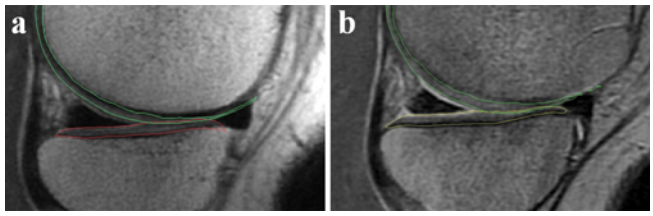

Fig. 4 Intersection volume between non-deformed tibiofemoral cartilage: (a) X-ray and supine MIR data (XSM); (b) Weight-bearing MRI (WBM)

2.4 In vivo subject-specific finite element model validation and verification

An iterative closet point algorithm (ICP) was used for alignment of X-ray and supine MRI data (XSM). The output of the ICP algorithm was a 4×4 transformation matrix that could be used to shift the bone between positions.[31] In order to reduce the error in six degrees of freedom in alignments of 2D and 3D images, X-rays were taken in coronal and sagittal views (Fig. 3). Deviation analysis for alignment error in 2D and 3D images was performed with Rapidform. This was similar to the technique used by Kurmis et al.[32] The model-predicted femoral cartilage-tibial cartilage contact areas were examined, and the intersection volume between non-deformed TF cartilage was characterized to determine the contact (Fig. 4). The cartilage contact deformation was then defined for each vertex of the articular surface mesh as the amount of cartilage surface penetration (mm) divided by the sum of the TF cartilage surface thicknesses. Cartilage contact deformation was calculated by determining the perpendicular distance

Table 1 The inter-observer reproducibility test result

	First observer	Second observer
Medial thickness		
Average CV (%)	1.6	1.2
Average thickness (mm)	2.67 ± 0.32	2.74 ± 0.29
Average SD (mm)	0.04 ± 0.02	0.03 ± 0.01
Lateral thickness		
Average CV (%)	1.9	1.3
Average thickness (mm)	3.36 ± 0.51	3.39 ± 0.41
Average SD (mm)	0.06 ± 0.02	0.04 ± 0.01

(CV, coefficient of variation; SD, standard deviation)

from the subchondral bone surface to the articular cartilage surface using Matlab (version 6.1; The MathWorks, Inc., Natick, MA, USA). Contact area determination was similar to the technique used for contact deformation. Weight-bearing is 70% of the subject's weight and subject-specific FE model was displacement-controlled by measuring kinematics under the weight-bearing MRI (WBM).[17]

3. Results

The 3D reconstruction reproducibility test conducted on healthy human cartilage demonstrated that inter-observer reproducibility was improved by using a rule-based approach to segmentation. The inter-observer reproducibility test showed good reproducibility (CV=1~2 %) for both thickness (Table 1).

To verify the results obtained using Rapidform, a deviation analysis of error from ICP algorithm in 2D and 3D alignment was conducted in a combined model. The average of points determined using each model were within 0.043 ± 0.011 mm and 0.021 ± 0.005 mm in coronal and sagittal views, respectively, validating the accuracy of alignment of the 2D and 3D images (Fig. 3).

The 3D reconstruction model developed in this study was accurate and precise. The XSM and WBM methods were employed for verification of the subject-specific FE model. The WBM method was the benchmark estimate for contact area and deformation, and the XSM method accurately predicted both of these measures. Both models showed good agreement in overlaying the predictions for contact area, and both were justified by comparison with the result from the WBM method (Fig. 5). Table 2 shows the values of contact area and contact deformation for subject specific XSM method, WBM method and FE model. The contact area in the medial articular cartilage was higher than that in the lateral articular cartilage, and the cartilage deformation was larger in the medial compartment than in the lateral compartment. In the subject-specific FE model, the contact area was 246.8 mm^2 and 188.5 mm^2 in the medial and lateral articular cartilages, respectively (Fig. 5). This relationship was consistent in both the XSM and WBM methods. The contact area on the lateral cartilage was 5.5 % different in the XSM method and 2.6 % different in the WBM compared to that in the subject-specific FE model, validating our subject-specific FE model. Once the subject-specific FE model was validated, cartilage deformation between the femoral and tibial cartilage and maximum cartilage deformation were extracted from the FE results, and these values were compared between the XSM and WBM methods. The

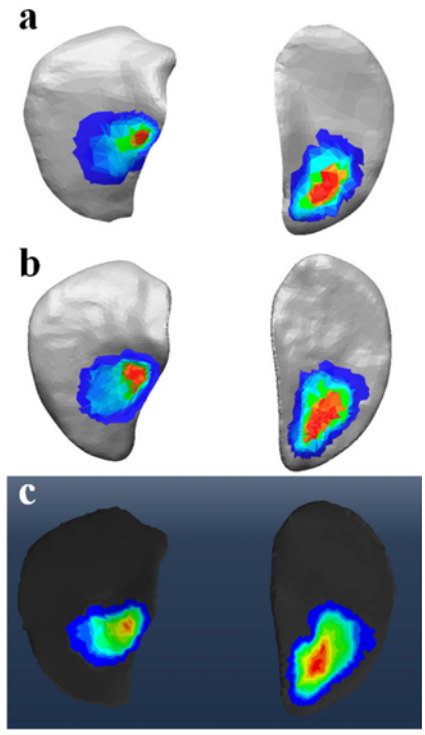

Fig. 5 Results of cartilage contact area and contact deformation distribution: (a) X-ray and supine MRI data (XSM); (b) Weight-bearing MRI (WBM); (c) Finite element model

Table 2 Result of cartilage contact area and contact deformation

	Contact area (mm^2)		Contact deformation (mm)	
	Medial	Lateral	Medial	Lateral
X-ray and supine MRI (XSM)	224.1	198.9	0.51	0.43
Weight-bearing MRI (WBM)	228.8	193.4	0.49	0.41
Finite element model	246.8	188.5	0.53	0.39

surfaces for cartilage deformation were measured in the distal femur and superior surface of the tibial cartilage. Peak cartilage deformation, in general, occurred in the medial compartment of both the femoral and tibial cartilages. Cartilage deformation was measured using the 3D models rather than the MRI contours. The total deformation of the contact area in the medial compartment was calculated at 0.49 mm using the cartilage geometry on the WBM method (Fig. 5). On the lateral side, the total deformation was calculated at 0.41 mm using the WBM method. Articular cartilage deformations were 0.53 mm and 0.39 mm in medial and lateral cartilages, respectively, according to the subject-specific FE model. The value of absolute deformation of lateral cartilage in the FE model compared to WBM was 0.02 mm and was 0.04 mm compared to the XSM method.

4. Discussion and Conclusions

The current study presents an innovative approach to *in vivo*

validation of subject-specific FE models of the knee joint. The subject-specific FE knee model used tissue-specific MRI scanning sequences and Mimics-based image processing to represent the 3D

geometry of knee joint tissues. The geometries of bone, meniscus, cartilage and ligaments influence the force and pressure values in the knee joint. Hence, the subject-specific FE knee model was created from 3D MRI and CT data-sets of an identical knee that was used for the *in vivo* experimental validation.

The importance of the verification of computational knee joint models has been emphasized by previous studies.[13-15,18] However, efforts toward *in vivo* FE modeling have been limited by difficulties in acquiring and analyzing multimodality data for model construction and validation, including proper co-registration and integration of required data. FE modeling of the TF is a very challenging mechanical problem mainly because of the uncertainty of validation data. Most of these models lack validation or verification against data from the same subjects.[4-8] The purpose of the present study was to apply easily adaptable validation methods to study the ability of a subject-specific FE model to reproduce close to the *in vivo* loading condition using the subject's own data. Verification was conducted by comparing the results from the model with either literature data or in vitro cadaveric data. However, specimens vary due to morphology variations across individuals, which lead to an unacceptable standard deviation in cadaver testing. Thus, conventional verification serves at best as a qualitative check. Moreover, cadaver testing is a high-cost method. In present, validations of FE study with results from its own cadaver test or outcomes published by others are still considered to be standard procedure in biomechanics. In our opinion, this could compromise the accuracy of predictions of the knee joint mechanical response and potentially obscure the true effects of structural alteration due to an injury or treatment when developing an implant. Currently, subject-specific implants are a challenging issue for many medical device companies. Recent evolution in computational technology allows FE studies to resolve non-linear, large deformation and contact problems so that we could mimic *in vivo* joint motions. Carey et al. used a dual fluoroscopy apparatus to validate their subject-specific data using kinematic analysis.[15] Therefore, an X-ray integration method using supine MRI was employed for the WBM method, as it does not require dual fluoroscopy but only X-ray and MRI, which are primary diagnostic techniques for patients undergoing general medical treatment.

In vivo measurements of joint pressure and stress continue to be a formidable challenge. We believe the contact area analysis using the XSM method proposed in this study offers a viable alternative for quantitative verification of subject-specific FE models based on *in vivo* data. 2-D X-ray has been used to measure *in vivo* knee joint kinematics because of its simplicity and accessibility.[33] In a previous study, a single, sagittal plane image 3D computer model of the knee joint was manipulated so that its projections on the image plane matched those captured during *in vivo* knee motion. The accuracy of this technique for accurate measurement of *in vivo* knee kinematics in six degrees of freedom is still controversial.[34]

Our study reduced the error in six degrees of freedom in alignments of 2D and 3D images. X-rays were taken in coronal and sagittal views. Furthermore, this algorithm was confirmed using Rapidform. The errors between the two images were 0.043 ± 0.011 and 0.021 ± 0.005 in coronal and sagittal views, respectively. The 3D reconstruction model developed in this study was accurate and precise due to the use of inter-observer studies. This study has also shown that the reproducibility of cartilage morphology measurements varies based on the observers during the subjective portion of the segmentation, and the accuracy of cartilage thickness measurement from MRI-derived 3D models is dependent on the region of interest on the cartilage.[30] Precision is an important consideration when using cartilage morphology measurement to evaluate cartilage thinning on a prospective basis. Inter-observer tests showed that each observer was highly consistent in segmenting articular cartilage from MRI images, comparable to other studies.[30, 35]

MRI images clearly indicate contact area and deformation on cartilage. Application of highly accurate task-specific kinematics is critical for achieving accurate subject-specific FE model predictions, as demonstrated by results from the current study. Creating a model in a weight-bearing state using non-weight-bearing kinematics introduces an artifact of joint congruity change, as evidenced by the differences in predicted contact area and contact deformation.[4] Once the validity of this method has been established, the model can be used with confidence to analyze the contact pressure and stress distribution in the joint complex. The XSM method used in this study is an acceptable validation method in general situations and showed very similar results to the WBM validation method for the *in vivo* model. In addition, although it applied different loading conditions compared to the weight-bearing FE model, the WBM model showed a trend similar to our subject-specific FE model.[12,14,15,26] The difference in contact deformation between benchmarked WBM and XSM methods was 0.02 mm and 0.02 mm in medial and lateral cartilages, respectively.

The present study has some limitations. First, the results were obtained with full extension of the knee. Different joint angles should be studied for verification and validation of our method. Second, the models were simulated under the only vertical loading condition, but more realistic boundary conditions including torsion and bending in knee joint would have to be considered in future. Third, material properties used in the current FE models were obtained from literature on subject-specific knee joint modeling, which may have contributed to the inaccuracy in contact area prediction. *In vivo* subject-specific material properties remain the target in biomechanics.[15] However, the ligaments play a central role in maintaining joint stability and therefore can influence the kinematics.[36] Therefore, the results of this study are valid and significant for future FE studies.

In conclusion, the XSM method proposed in this study represents a step forward in subject-specific *in vivo* validation of original subjects in biomechanics. The approach outlined introduces a generic validation tool for the study of *in vivo* knee joint behavior. Future studies should focus on verification methods of material properties for subject-specific *in vivo* models.

REFERENCES

1. Elias, J. J., Wilson, D. R., Adamson, R., and Cosgarea, A. J., "Evaluation of a Computational Model Used to Predict the

Patellofemoral Contact Pressure Distribution," Journal of Biomechanics, Vol. 37, No. 3, pp. 295-302, 2004.

2. Andriacchi, T. P. and Alexander, E. J., "Studies of Human Locomotion: Past, Present and Future," Journal of Biomechanics, Vol. 33, No. 10, pp. 1217-1224, 2000.
3. Anderson, A. E., Ellis, B. J., and Weiss, J. A., "Verification, Validation and Sensitivity Studies in Computational Biomechanics," Computer Methods in Biomechanics and Biomedical Engineering, Vol. 10, No. 3, pp. 171-184, 2007.
4. Bao, H. R. C., Zhu, D., Gong, H., and Gu, G. S., "The Effect of Complete Radial Lateral Meniscus Posterior Root Tear on the Knee Contact Mechanics: A Finite Element Analysis," Journal of Orthopaedic Science, Vol. 18, No. 2, pp. 256-263, 2013.
5. Kwon, O. R., Kang, K. T., Son, J., Kwon, S. K., Jo, S. B., et al., "Biomechanical Comparison of Fixed-and Mobile-Bearing for Unicomparmental Knee Arthroplasty Using Finite Element Analysis," Journal of Orthopaedic Research, Vol. 32, No. 2, pp. 338-345, 2014.
6. Chen, C. S., Cheng, C. K., Liu, C. L., and Lo, W. H., "Stress Analysis of the Disc Adjacent to Interbody Fusion in Lumbar Spine," Medical engineering & Physics, Vol. 23, No. 7, pp. 485-493, 2001.
7. Kim, H. J., Chun, H. J., Kang, K. T., Lee, H. M., Kim, H. S., et al., "A Validated Finite Element Analysis of Nerve Root Stress in Degenerative Lumbar Scoliosis," Medical & Biological Engineering & Computing, Vol. 47, No. 6, pp. 599-605, 2009.
8. Quatman, C. E., Kiapour, A., Myer, G. D., Ford, K. R., Demetropoulos, C. K., et al., "Cartilage Pressure Distributions Provide a Footprint to Define Female Anterior Cruciate Ligament Injury Mechanisms," The American Journal of Sports Medicine, Vol. 39, No. 8, pp. 1706-1713, 2011.
9. Baldwin, M. A., Clary, C., Maletsky, L. P., and Rullkoetter, P. J., "Verification of Predicted Specimen-Specific Natural and Implanted Patellofemoral Kinematics during Simulated Deep Knee Bend," Journal of Biomechanics, Vol. 42, No. 14, pp. 2341-2348, 2009.
10. Fukubayashi, T. and Kurosawa, H., "The Contact Area and Pressure Distribution Pattern of the Knee: A Study of Normal and Osteoarthrotic Knee Joints," Acta Orthopaedica, Vol. 51, No. 1-6, pp. 871-879, 1980.
11. Anderson, A. E., Ellis, B. J., Maas, S. A., Peters, C. L., and Weiss, J. A., "Validation of Finite Element Predictions of Cartilage Contact Pressure in the Human Hip Joint," Journal of Biomechanical Engineering, Vol. 130, No. 5, Paper No. 051008, 2008.
12. Beillas, P., Papaioannou, G., Tashman, S., and Yang, K., "A New Method to Investigate in Vivo Knee Behavior using a Finite Element Model of the Lower Limb," Journal of Biomechanics, Vol. 37, No. 7, pp. 1019-1030, 2004.
13. Beillas, P., Lee, S. W., Tashman, S., and Yang, K., "Sensitivity of the Tibio-Femoral Response to Finite Element Modeling Parameters," Computer Methods in Biomechanics and Biomedical Engineering, Vol. 10, No. 3, pp. 209-221, 2007.
14. Yao, J., Salo, A. D., Lee, J., and Lerner, A. L., "Sensitivity of Tibio-Menisco-Femoral Joint Contact Behavior to Variations in Knee Kinematics," Journal of Biomechanics, Vol. 41, No. 2, pp. 390-398, 2008.
15. Carey, R. E., Zheng, L., Aiyangar, A. K., Harner, C. D., and Zhang, X., "Subject-Specific Finite Element Modeling of the Tibiofemoral Joint Based on CT, Magnetic Resonance Imaging and Dynamic Stereo-Radiography Data in Vivo," Journal of Biomechanical Engineering, Vol. 136, No. 4, Paper No. 041004, 2014.
16. Willén, J., Danielson, B., Gaulitz, A., Niklason, T., Schönström, N., and Hansson, T., "Dynamic Effects on the Lumbar Spinal Canal: Axially Loaded CTMyelography and MRI in Patients with Sciatica and/or Neurogenic Claudication," Spine, Vol. 22, No. 24, pp. 2968-2976, 1997.
17. Ramappa, A. J. and Bansal, P., "Correlation of Patellofemoral Maltracking and Anterior Knee Pain," http://www.orthojournalhms.org/volume7/pdfs/ms09.pdf (Accessed 15 MAY 2015)
18. Pena, E., Calvo, B., Martinez, M., and Doblare, M., "A Three-Dimensional Finite Element Analysis of the Combined Behavior of Ligaments and Menisci in the Healthy Human Knee Joint," Journal of Biomechanics, Vol. 39, No. 9, pp. 1686-1701, 2006.
19. Shepherd, D. and Seedhom, B., "The 'instantaneous' Compressive Modulus of Human Articular Cartilage in Joints of the Lower Limb," Rheumatology, Vol. 38, No. 2, pp. 124-132, 1999.
20. Dhaher, Y. Y., Kwon, T. H., and Barry, M., "The Effect of Connective Tissue Material Uncertainties on Knee Joint Mechanics under Isolated Loading Conditions," Journal of Biomechanics, Vol. 43, No. 16, pp. 3118-3125, 2010.
21. Donahue, T. L. H., Hull, M., Rashid, M. M., and Jacobs, C. R., "How the Stiffness of Meniscal Attachments and Meniscal Material Properties Affect Tibio-Femoral Contact Pressure Computed using a Validated Finite Element Model of the Human Knee Joint," Journal of Biomechanics, Vol. 36, No. 1, pp. 19-34, 2003.
22. Yang, N. H., Canavan, P. K., and Nayeb-Hashemi, H., "The Effect of the Frontal Plane Tibiofemoral Angle and Varus Knee Moment on the Contact Stress and Strain at the Knee Cartilage," Journal of Applied Boimechanical, Vol. 26, No. 4, pp. 432-443, 2010.
23. Zielinska, B. and Donahue, T. L. H., "3D Finite Element Model of Meniscectomy: Changes in Joint Contact Behavior," Journal of Biomechanical Engineering, Vol. 128, No. 1, pp. 115-123, 2006.
24. Guess, T. M., Thiagarajan, G., Kia, M., and Mishra, M., "A Subject Specific Multibody Model of the Knee with Menisci," Medical Engineering & Physics, Vol. 32, No. 5, pp. 505-515, 2010.
25. Mow, V. C., Ateshian, G. A., and Spilker, R. L., "Biomechanics of Diarthrodial Joints: A Review of Twenty Years of Progress," Journal of Biomechanical Engineering, Vol. 115, No. 4B, pp. 460-467, 1993.
26. LaPrade, R. F., Engebretsen, A. H., Ly, T. V., Johansen, S., Wentorf, F. A., and Engebretsen, L., "The Anatomy of the Medial Part of the Knee," The Journal of Bone & Joint Surgery, Vol. 89, No. 9, pp.

2000-2010, 2007.

27. LaPrade, R. F., Morgan, P. M., Wentorf, F. A., Johansen, S., and Engebretsen, L., "The Anatomy of the Posterior Aspect of the Knee. An Anatomic Study," Journal of Bone Joint Surgery. American Volume, Vol. 89, No. 4, pp. 758-764, 2007.

28. Mesfar, W. and Shirazi-Adl, A., "Biomechanics of the Knee Joint in Flexion under Various Quadriceps Forces," The Knee, Vol. 12, No. 6, pp. 424-434, 2005.

29. Takeda, Y., Xerogeanes, J. W., Livesay, G. A., Fu, F. H., and Woo, S. L., "Biomechanical Function of the Human Anterior Cruciate Ligament," Arthroscopy: The Journal of Arthroscopic & Related Surgery, Vol. 10, No. 2, pp. 140-147, 1994.

30. Koo, S., Gold, G., and Andriacchi, T., "Considerations in Measuring Cartilage Thickness using MRI: Factors Influencing Reproducibility and Accuracy," Osteoarthritis and Cartilage, Vol. 13, No. 9, pp. 782-789, 2005.

31. Besl, P. J. and McKay, N. D., "Method for Registration of 3-D Shapes," Proc. of SPIE, Vol. 1611, pp. 586-606, 1992.

32. Kurmis, A. P., Hearn, T. C., Field, J. R., Grimmer, K., and Reynolds, K. J., "The Accuracy of Three-Dimensional Reconstructions of the Ovine Knee: Dissectional Validation," Computerized Medical Imaging and Graphics, Vol. 26, No. 3, pp. 171-175, 2002.

33. You, B. M., Siy, P., Anderst, W., and Tashman, S., "In Vivo Measurement of 3-D Skeletal Kinematics from Sequences of Biplane Radiographs: Application to Knee Kinematics," IEEE Transactions on Medical Imaging, Vol. 20, No. 6, pp. 514-525, 2001.

34. Komistek, R. D., Dennis, D. A., and Mahfouz, M., "In Vivo Fluoroscopic Analysis of the Normal Human Knee," Clinical Orthopaedics and Related Research, Vol. 410, pp. 69-81, 2003.

35. Eckstein, F., Heudorfer, L., Faber, S., Burgkart, R., Englmeier, K.-H., and Reiser, M., "Long-Term and Resegmentation Precision of Quantitative Cartilage MR Imaging (qMRI)," Osteoarthritis and Cartilage, Vol. 10, No. 12, pp. 922-928, 2002.

36. Woo, S. L., Debski, R. E., Withrow, J. D., and Janaushek, M. A., "Biomechanics of Knee Ligaments," The American Journal of Sports Medicine, Vol. 27, No. 4, pp. 533-543, 1999.